Electronic Supplementary Material (ESI) for RSC Advances.

SUPPLEMENTARY INFORMATION

Low Temperature Atomic Layer Deposition of Zirconium Oxide for Inkjet Printed Transistor Applications

Mohi Uddin Jewel,[1] MD Shamim Mahmud,[1] Mahmuda Akter Monne,[2] Alex Zakhidov, [2,3] and Maggie Yihong Chen[1,2,a)]

[1]Ingram School of Engineering, Texas State University, San Marcos, Texas 78666, USA

[2]Materials Science, Engineering, and Commercialization, Texas State University, San Marcos, Texas 78666, USA

[3]Department of Physics, Texas State University, San Marcos, Texas 78666, USA

Atomic Layer Deposition (ALD) of Zirconium Oxide (ZrO_2):

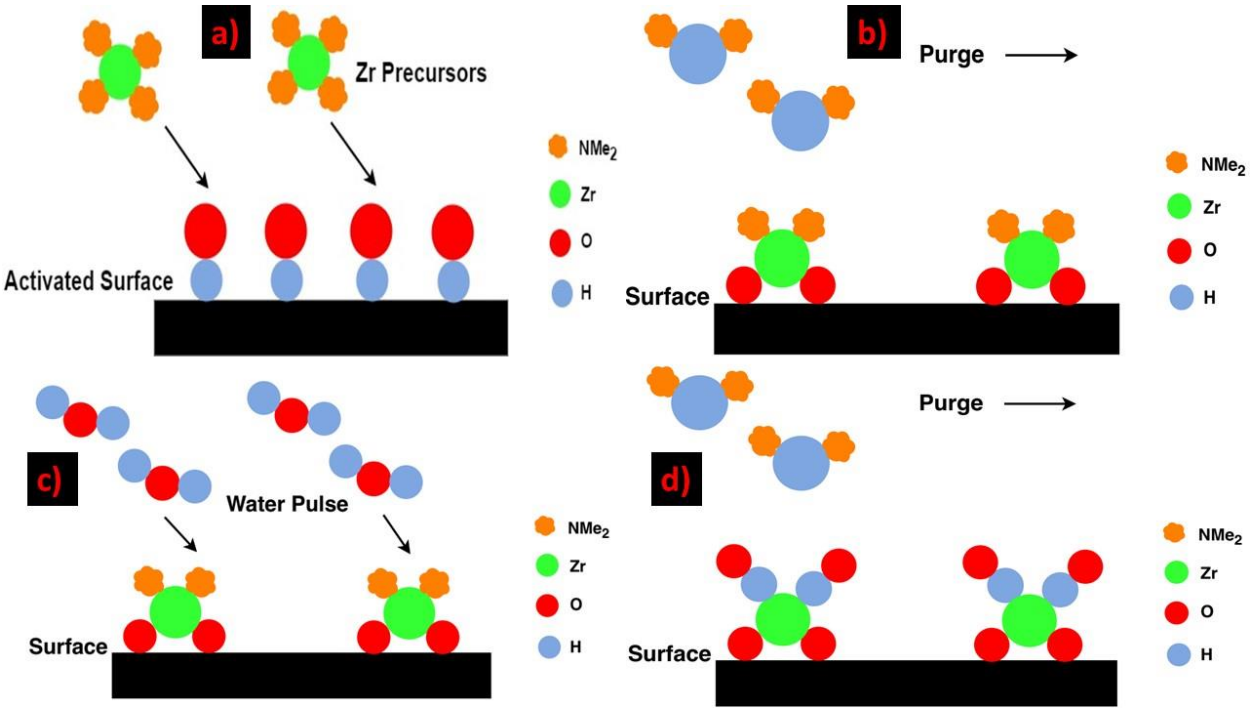

Figure S1. Diagram for single ALD-ZrO_2 cycle – a) 400 ms dose of TDMAZr, b) 20 s argon gas purge of excess TDMAZr and byproducts, c) 50 ms dose of H_2O, and d) 20 s argon purge of excess water and byproducts.

Atomic force microscopy (AFM) and scanning electron microscopy images of the 2D ALD-ZrO_2 surface:

The variation of the surface structure at different temperatures due to crystallinity change is illustrated with the 2D AFM images in Figure S2a-c for 300 ALD cycles. At 150 ^oC, there are few

bulges on the amorphous surface while few dents are observed on the partially and fully crystalline surface at 200 and 250 ^{o}C. The surface at 200 ^{o}C was quite homogeneous with no obvious crystal facets, which is shown in the SEM image of Figure S2d.

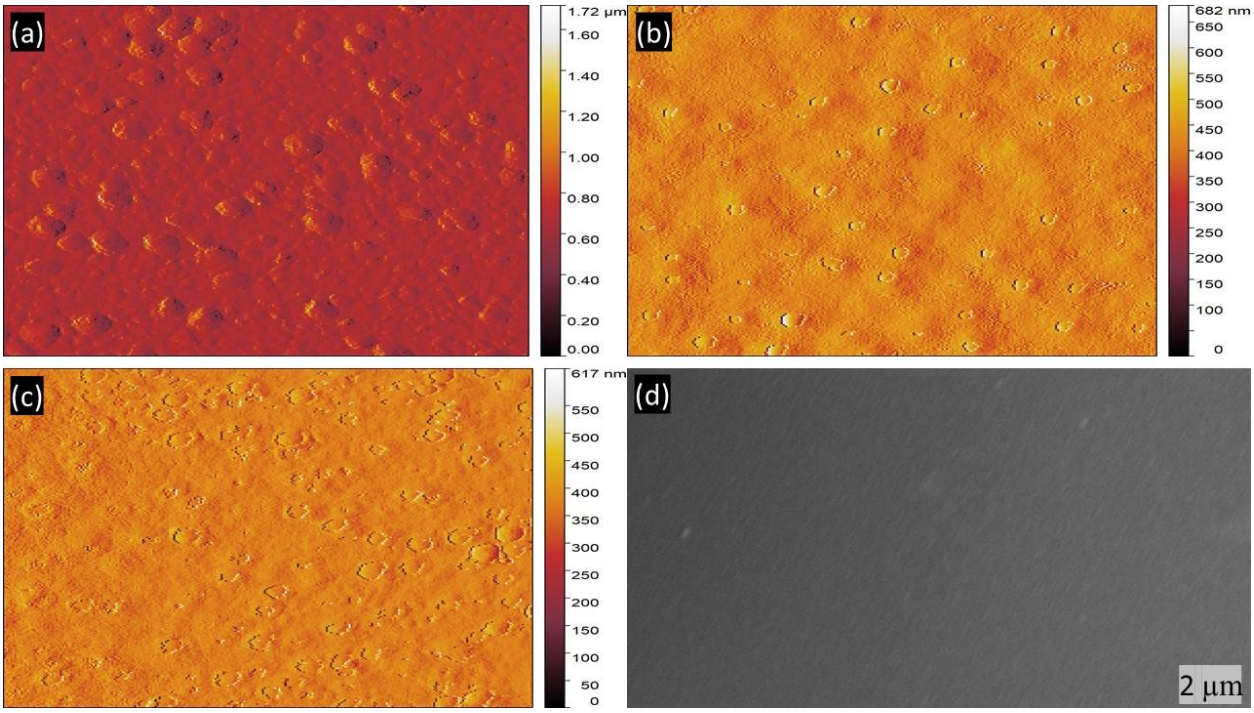

Figure S2. 2D AFM images of ZrO_2 of thickness - (a) 38.58 nm grown at 150 ^{o}C, (b) 32.51 nm grown at 200 ^{o}C, (c) 22.2 nm prepared at 250 ^{o}C; (d) An SEM image of 46.4 nm thick ZrO_2 grown at 200 ^{o}C.

Energy- dispersive spectra (EDS) of ALD – ZrO_2:

Energy-dispersive spectra (EDS) reveals no chemical contamination of the films i.e. with other chemical elements (see Figure S3). Microanalysis is done with NIST DTSA II software (D.E. Newbury, N.W.M. Ritchie, Journal of Materials Science, 50(2), 493–518 (2015). reveals, the weight ratio of Zr : O is around 21 : 8 with statistical deviation of 6%. Si K dominating peak at 1.74 eV comes from the Si substrate.

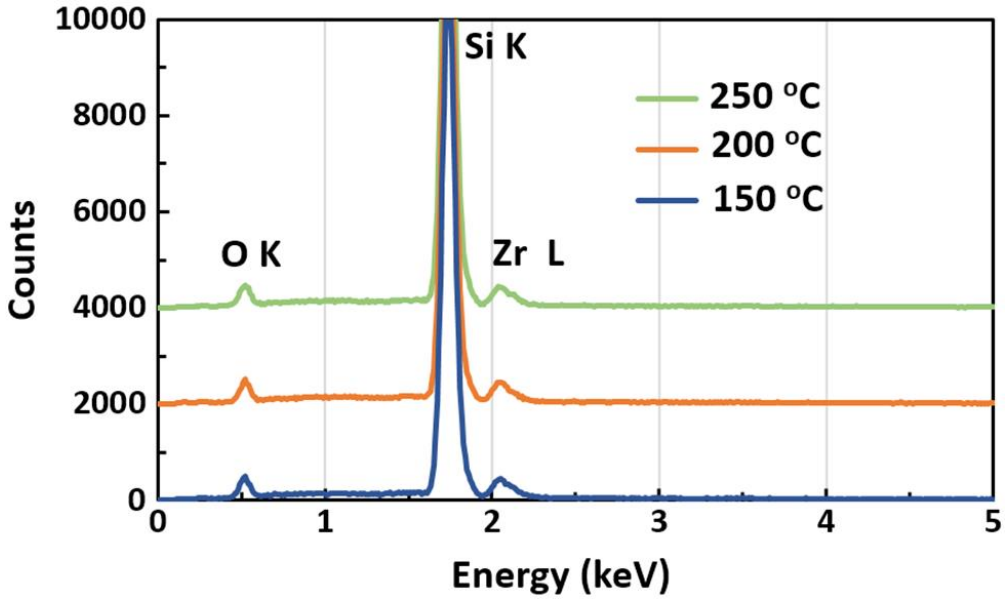

Figure S3. Energy-dispersive spectra (EDS) of the ALD – ZrO_2 films grown at different temperatures.

Hysteresis in the ALD-ZrO_2 dielectric:

The hysteresis behavior of the ALD-ZrO_2 was examined for a 21.17 nm sample grown at 200 °C. Initially the voltage was swept in forward (negative to positive) direction, then in reverse (positive to negative) direction as indicated in Figure S4. The oxide has small hysteresis.

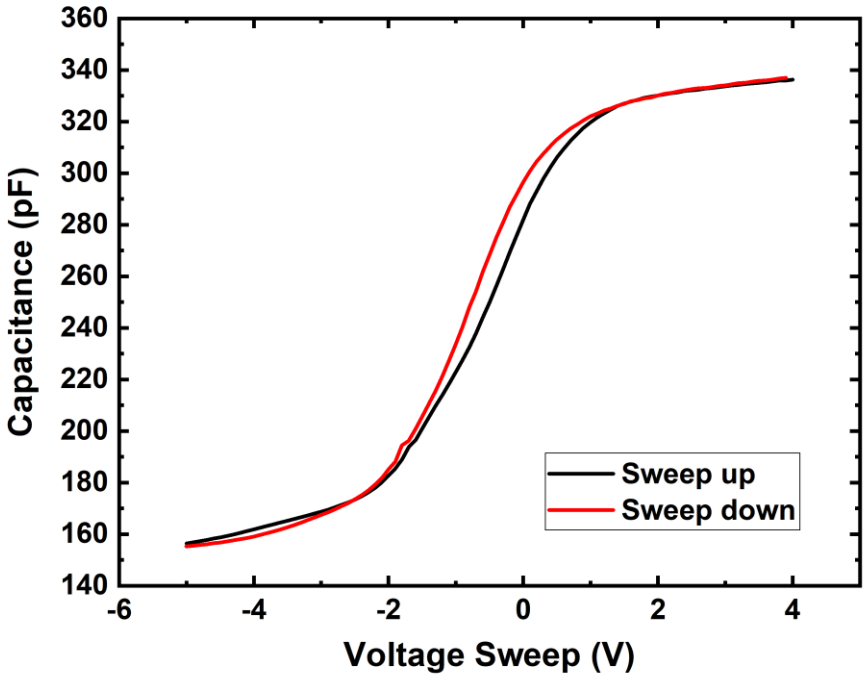

Figure S4. Hysteresis in an ALD-ZrO_2 of thickness 21.17 nm grown at 200 °C.

Graphene ink preparation and characterization:

For a 10 mL of graphene ink, terpineol/cyclohexanone with a ratio of 1.5/8.5 was mixed with a stabilizing polymer i.e. ethyl cellulose of 16 mg, and sonicated (Branson 2510) for 1 hour. About 1.6 mg of graphene powder was dispersed into the solution and sonicated for 10 ~ 20 hours. The mixture was then centrifuged at 5000 rpm for 30 minutes and left to rest overnight. The supernatant was collected by pipetting and ready for further use. The viscosity and surface tension of our graphene ink was ~5.5 mPa.s and ~ 29 mN/ m, which is suitable for inkjet printing.[1]

Once the ink is ready, it is useful to know the concentration of graphene nanoflakes in the ink. A Shimadzu UV-2501 spectrophotometer was used to obtain the absorbance spectra of graphene ink. Figure S5a shows the absorbance spectra of graphene ink diluted to 10% in isopropanol to avoid scattering losses. The Beer-Lambert law can be expressed as $A = \alpha cl$, where A is the absorbance, α is the absorption coefficient ($Lg^{-1}m^{-1}$), c is the concentration of dispersed graphene (g/L), and l is the light path length (m). Using the Beer-Lambert law at the wavelength $\lambda = 660$ nm, it is possible to calculate the concentration of graphene from the absorbance spectra. From $A = 0.201$, $\alpha = 2460$ $Lg^{-1}m^{-1}$, $l = 0.01$ m, our estimated graphene concentration is 0.08 mg/mL.[2]

Raman spectroscopy is a strong tool for characterizing the carbon materials such as diamond, carbon nanotube, and graphene. The underlying insulator surface chemistry can affect the Raman spectroscopy of graphene through surface-graphene interaction.[3] Moreover, Raman measurement is an excellent way to find appropriate solvents for ink by visualizing the solvent-induced disorder in graphene nanosheets. Inset of Figure S5b shows an inkjet printed graphene pattern of area 620 × 740 μm^2 on ALD-ZrO_2 surface using a Fujifilm Dimatix Materials Printer (DMP 2800). The inkjet printer can create a predefined pattern on a ZrO_2 surface. Several patterns were printed on ZrO_2/Si and cured at 375 ^oC. Figure S5b plots the Raman spectra of annealed samples. A signature of graphene, the intense G, and 2D peaks were observed at around 1570 and 2687 cm^{-1} respectively. A low-intensity D peak has appeared at ~1358 cm^{-1} which is associated with the disorder in the graphene.[4] The intensity ratios I_D/I_G of 0.086 and 0.122 indicate the low amount of solvent, and ZrO_2 induced disorder, and good quality of graphene flakes. Terpineol/cyclohexanone and ethyl cellulose can be ideal solvents and surfactant for graphene-based inks. It is clear from G and 2D peaks that the thin films have few-layer graphene flakes. The discrepancy in the wave

number of ~2 cm^{-1} between the Raman spectra reveals non-homogeneity in graphene flakes, and separate interaction mechanisms between graphene and ALD-ZrO_2.

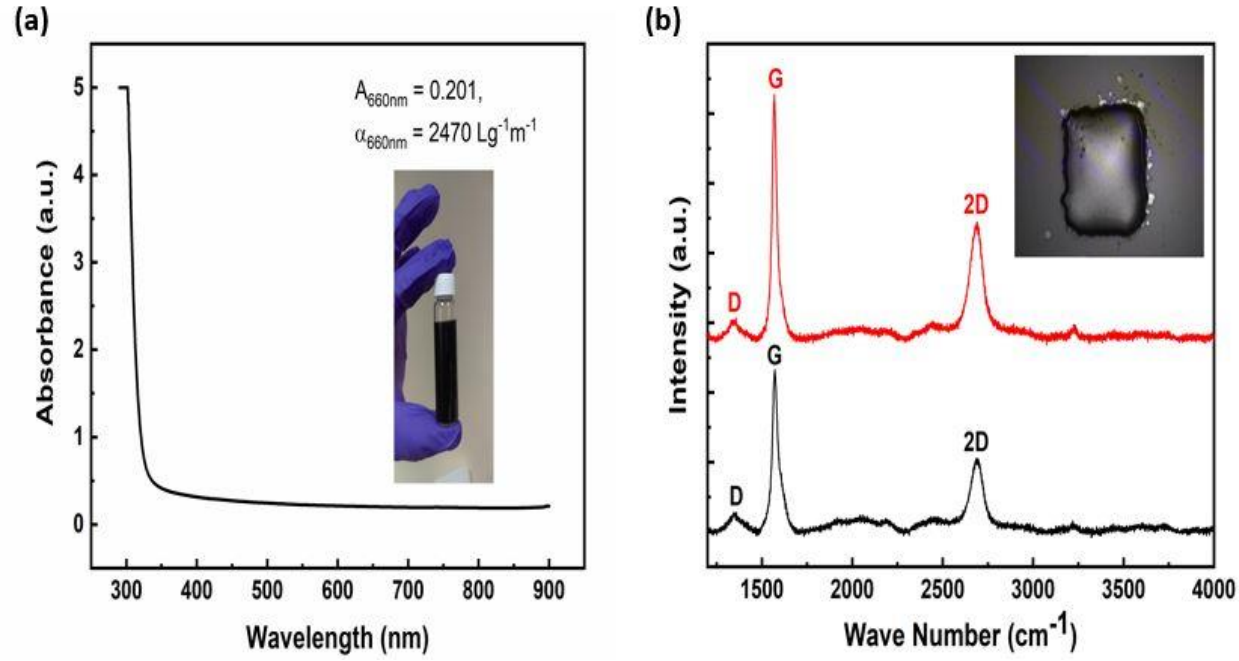

Figure S5. a) Absorbance spectrum of graphene ink. Inset shows graphene ink. b) Raman spectrum of inkjet printed graphene. Inset shows inkjet printed graphene on ZrO_2 surface.

Transfer characteristics of printed graphene transistor:

The transfer curves are shown for various drain voltages. The change in the drain current is obvious from the transfer curves.

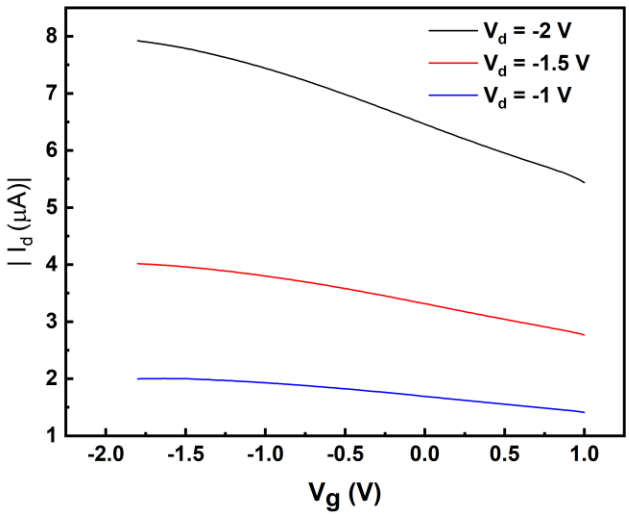

Figure S6. Transfer curves of printed graphene transistor.

References:

1 E. B. Secor, P. L. Prabhumirashi, K. Puntambekar, M. L. Geier and M. C. Hersam, *J. Phys. Chem. Lett.*, 2013, **4**, 1347–1351.

2 T. Hasan, F. Torrisi, Z. Sun, D. Popa, V. Nicolosi, G. Privitera, F. Bonaccorso and A. C. Ferrari, *Phys. Status Solidi Basic Res.*, 2010, **247**, 2953–2957.

3 T. Tsukamoto, K. Yamazaki, H. Komurasaki and T. Ogino, *J. Phys. Chem. C*, 2012, **116**, 4732–4737.

4 A. C. Ferrari, *Solid State Commun.*, 2007, **143**, 47–57.